Journal of Molecular Liquids 307 (2020) 112989

Contents lists available at ScienceDirect

Journal of Molecular Liquids

journal homepage: www.elsevier.com/locate/molliq

A novel amphipathic low-melting complex salt: An efficient homogeneous catalyst for synthesis of pyran-annulated heterocyclic scaffolds and pyrido[2,3-*d*]pyrimidines

Maedeh Saeedi Mirak-Mahaleh, Kurosh Rad-Moghadam *

Department of Chemistry, University of Guilan, Rasht, PO Box 41335-1914, Iran

ARTICLE INFO

Article history:
Received 1 December 2019
Received in revised form 2 March 2020
Accepted 23 March 2020
Available online 25 March 2020

Keywords:
Amphipathic mixed salt
Benzo[*b*]pyrans
Pyrano[3,2-*c*]quinolines
Pyrido[2,3-*d*]pyrimidines
Homogeneous catalysis
Acidic ionic liquid

ABSTRACT

The reaction of triethyl(sulfonyl)ammonium chlorosulfonate with 1,1,3,3-tetramethylguanidine (TMG) gave a low-melting complex salt with amphipathic and acidic characters. The salt has a great tendency towards solvation of organic substrates upon slight heating, so it was employed as a homogeneous acidic and functional ionic liquid catalyst in the expedient synthesis of benzo[*b*]pyrans, pyrano[4,3-*b*]pyrans, pyrano[3,2-*c*]quinolones, and pyrido[2,3-*d*]pyrimidines. The catalytic activity of the complex salt is much better than the simple salts composing it. Spectroscopic studies and chemical analysis of the salt revealed that its empirical formula is in agreement with neutralization of TMG by two H_2SO_4 molecules. The HSO_4^- anions of the salt seem to form extensive H-bonding with the constituting ammonium cations and Cl^-, resulting in melting point depression of the complex salt due to the melting points of pure triethylamine and TMG hydrochloride salts. Another significant feature of this solid salt is that it can preserve its composition even after several times of separation from aqueous extracts and can be handled easily without danger.

1. Introduction

Right after their emergence as neoteric solvents, ionic liquids (ILs) drew a lot research attention in green chemistry. The intrinsic properties of ILs such as non-flammability, negligible vapor pressure, favorable solvation behavior, recyclability, and high thermal stability make them ideal replacements for the noxious organic volatile solvents [1–4]. Since ILs are salts of bulky organic ions, they melt at near room temperature and can establish van der Waals, dipole-dipole, and electrostatic attractions with the reacting species including the reaction transition states, leading to possible reaction rate enhancement. In addition to promoting some reactions on their own [5], ILs can be functionalized on their organic cations or anions to carry out specific catalytic activities [6,7]. Although a wide variety of organic salts are available, only a limited array of them melt at near room temperature. Indeed, the lattice energy for most of these salts is too high to be overcome by the thermal energy of the molecules at near ambient temperatures. Making interruptions in the lattice structure of a high-melting IL by doping it with an auxiliary salt is a recent strategy to extend the scope of low-melting ILs while maintaining the whole ionic characteristic of the resulting mixture. Most of the thus far reported IL mixtures have been prepared by fusion of two organic salts [8,9]. The binary ionic liquid mixtures (BILs) formed in this way contain the ions which are intended to play as catalyst in a reaction and the ions of the co-melting salt. It is believed that BIL mixtures have supramolecular structures even in the liquid state [10,11], however with smaller sizes and perhaps different orders of ions relative to their constituting salts. Certainly, these structural features give the IL mixtures new physicochemical properties in addition to melting point depression and decreased viscosity as compared to their constituent pure salts. Inspired by this background, we recently reported the preparation of a typically uncommon BIL by doping 1,1,3,3-tetramethylguanidine hydrochloride [TMG-H]Cl (Mp ~210 °C) with a zwitterionic molecule [12]. In the present study, a low-melting mixed hydrogensulfate and hydrochloride salt of 1,1,3,3-tetramethylguanidine and triethylamine is introduced. Due to the fact that it is amphipathic, the novel complex salt (CS) can form homogeneous solutions with organic substrates at temperatures lower than 100 °C. Thus, because of its functional and acidic nature, we examined it as the catalyst in the synthesis of some pyran annulated heterocycles and pyrido[2,3-*d*]pyrimidines. Much research attention has been paid to the development of one-pot synthesis of benzo[*b*]pyrans, pyrano[4,3-*b*]pyrans, pyrano[3,2-*c*]quinolones, and pyrido[2,3-*d*]pyrimidines [13–17], since these compounds have shown interesting pharmaceutical and biological properties such as antiallergenic [18], anti-inflammatory [19], antitumor [20], anticonvulsant [21], antitubercular [22], antimalarial [23], and antihyperglycemic [24] activities. Consequently, various methods based on using different catalysts have been

* Corresponding author.
E-mail address: radmm@guilan.ac.ir (K. Rad-Moghadam).

https://doi.org/10.1016/j.molliq.2020.112989
0167-7322/

developed for the synthesis of these compounds. Despite numerous merits of the recent synthetic methods [25–33] some suffer from one or more impediments such as poor product yields, extended reaction time, unreusability of the catalysts, and pollution of the environment. We show that these issues can be addressed by using the complex salt as the catalyst in the three-component synthesis of the above compounds.

2. Experimental section

2.1. Materials and instruments

All chemicals were purchased from Merck and Sigma-Aldrich companies and used without any further purification. All the products are known compounds and were identified by comparing their melting points and spectral data with those of authentic samples. The progress of the reactions was monitored by thin layer chromatography (TLC) using silica gel SILG/UV 254 plates. Melting points (mp) were measured on a Buchi B-545 apparatus and are uncorrected. The ^{1}H NMR (400 MHz) spectra were recorded in DMSO-d_6 on a Bruker DRX-400 spectrometer. The Fourier transform infrared (FT-IR) spectra were taken in KBr pellets on a Shimadzu FT-IR 8300 spectrometer in the range of 400–4000 cm^{-1}. The TGA (thermogravimetric analysis) and DSC (differential scanning calorimetry) studies of the complex salt were conducted under He atmosphere on a SETARAM thermal analyzer at a heating rate of 20 °C/min from 25 to 600 °C. Electric conductivities were performed by an Orion 101 conductometer using a platinum conductivity cell (cell constant = 1 cm^{-1}).

2.2. Preparation of the complex salt [TMG-H][Et$_3$N-H][(HCl)(HSO$_4$)$_2$]

The first step of this preparation is based on a modified procedure [34]. Thus, to an ice-cooled flask (50 mL) containing a magnetic stirring bar and a solution of triethylamine (0.50 g, 5 mmol) in dry CH_2Cl_2 (8 mL) was added dropwise a solution of chlorosulfonic acid (0.66 mL, 10 mmol) in dry CH_2Cl_2 (3 mL) over a period of 10 min at 0 °C. Stirring was continued after the addition for 4 h, during which the reaction mixture was allowed to warm to room temperature. Evaporation of the solvent under reduced pressure at 50 °C gave [Et$_3$N–SO$_3$H]ClSO$_3$ as a viscous pale yellow oil (Fig. 1). This oil was dissolved in CH_2Cl_2 (4 mL) and to the resulting solution was added dropwise 1,1,3,3-tetramethylguanidine (0.625 mL, 5 mmol) in CH_2Cl_2 (2 mL) and then the mixture was stirred in air at ambient temperature for 4 h. The white powdery solid of [TMG-H][Et$_3$N-H][(HCl)(HSO$_4$)$_2$] was obtained in 98% yield by decanting the solvent and drying the solid under reduced pressure at 40 °C.

Selected spectral data for [TMG-H][Et$_3$N-H][(HCl)(HSO$_4$)$_2$]:

Table 1
Solubility tests for the CS in common selected solvents.

Solvent	At 25 °C	Hot[a]
CH_2Cl_2	Insoluble	Less soluble
$CHCl_3$	Insoluble	Less soluble
H_2O	Soluble	Soluble
EtOH	Soluble	Soluble
DMSO	Soluble	Soluble
AcOEt	Insoluble	Paste
THF	Insoluble	Paste

[a] At the boiling points of the selected solvents.

IR (KBr): υ_{max} (cm^{-1}) 595, 879, 1058, 1191, 1220, 1470, 1613, 1648, 2940, 2973, 3377. ^{1}H NMR (400 MHz, DMSO-d_6): δ_H 1.21 (9H, t, J 7.2 Hz, 3 CH_3), 2.91 (12H, s, 2 N(CH_3)$_2$), 3.08 (6H, p, J 6.8 Hz, 3 CH_2), 5.95 (3H, broad s, 2 HSO_4 and HCl), 7.88 (2H, s, =NH_2), 9.82 (1H, s, Et$_3$N<u>H</u>).

Information about solubility of the CS is more important when searching for an appropriate separation procedure during workup of the reaction mixtures. Thus, the solubility of the CS in several common solvents was determined and the results are given in Table 1.

2.3. General procedure for the one-pot preparation of benzo[b]pyrans, pyrano[4,3-b]pyrans, pyrano[3,2-c]quinolones, and pyrido[2,3-d]pyrimidines under catalysis of the ionic liquid [TMG-H][TEA-H][(HCl)(HSO$_4$)$_2$]

To a vial (10 mL) containing a β-dicarbonyl compound (4-hydroxycoumarin/ dimedone/ 4-hydroxy-6-methyl-2-pyrone/ 4-hydroxyquinolin-2-one) or 6-aminouracil (1 mmol) were added malononitrile (1.1 mmol), an arylaldehyde (1 mmol), a magnetic stirring bar, and the salt [TMG-H][Et$_3$N-H][(HCl)(HSO$_4$)$_2$] (0.1 mmol, 0.045 g). The mixture was magnetically stirred under solvent-free condition at 70 °C for an appropriate period of time (according to Table 3). After completion of the reaction, as monitored by TLC on silica gel using a 1:1 ethyl acetate/n-hexane mixture, distilled water (5 mL) was added, while stirring, to the reaction mixture. The precipitated crude product was separated by filtration from the aqueous layer and purified by washing with water and recrystallization from ethanol (95%). For separation of the salt, the filtrates of several experiments were combined and then evaporated at 50 °C under reduced pressure. The salt remaining after evaporation of the water was collected for reuse.

2.4. The spectral data of selected compounds

2-Amino-4-(4-chlorophenyl)-5-oxo-5,6-dihydro-4*H*-pyrano[3,2-*c*]quinoline-3-carbonitrile **8c**:

IR (KBr) υ_{max} (cm^{-1}): 1383 (C—O pyran), 1674 (C=O), 2187 (C≡N), 3169, 3286, 3379, 3408 (N—H). ^{1}H NMR (400.13 MHz,

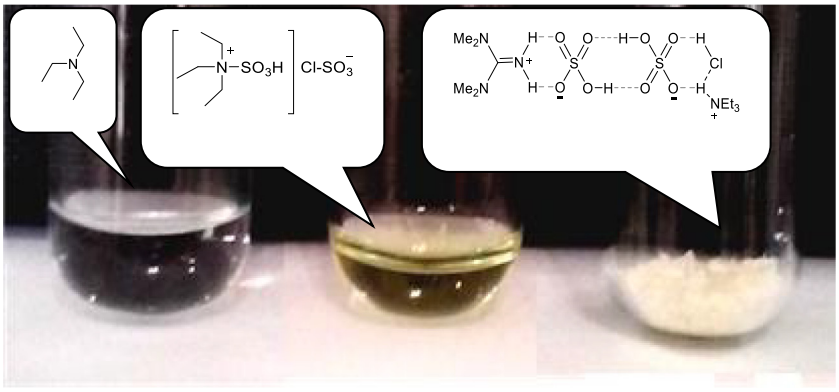

Fig. 1. Steps in production of [TMG-H][Et$_3$N-H][(HCl)(HSO$_4$)$_2$].

DMSO-d_6): δ_H 4.52 (1H, s, 4-H), 7.24 (2H, d, *J* 8.4 Hz 2′- and 6′-H), 7.30 (1H, dt, *J* 8.0 and 1.2 Hz, 9-H), 7.32 (2H, s, NH_2), 7.34 (1H, d, *J* 8.4 Hz, 7-H), 7.35 (2H, d, *J* 8.4 Hz, 3′-H and 5′-H), 7.59 (1H, dt, *J* 7.8 and 1.2 Hz, 8-H), 7.91 (1H, dd, *J* 8.0 and 1.2 Hz, 10-H), 11.80 (1H, s, N—H).

2-Amino-4-(4-nitrophenyl)-5-oxo-5,6-dihydro-4*H*-pyrano[3,2-*c*] quinoline-3-carbonitrile **8e:**

IR (KBr) υ_{max} (cm^{-1}): 1348 and 1514 (NO_2), 1387, 1632, 1674, 2202 (C≡N), 3335 and 3406 (N—H). ^{1}H NMR (400.13 MHz, DMSO-d_6): δ_H 4.69 (1H, s, 4-H), 7.31 (1H, t, *J* 7.6 Hz, 9-H), 7.34 (1H, d, *J* 9.2 Hz, 7-H), 7.42 (2H, s, NH_2), 7.51 (2H, d, *J* 8.8 Hz, 2′- and 6′-H), 7.60 (1H, dt, *J* 7.8 and 1.2 Hz, 8-H), 7.93 (1H, d, *J* 8.0 Hz, 10-H), 8.17 (1H, d, *J* 8.8 Hz, 3′-H and 5′-H), 11.84 (1H, s, N H).

2-Amino-4-(4-methoxyphenyl)-5-oxo-5,6-dihydro-4*H*-pyrano[3,2-*c*]quinoline-3-carbonitrile **8f**: IR (KBr) υ_{max} (cm^{-1}): 1379 (C—O pyran), 1632 (N—H bend), 1676 (C═O), 2183 (C≡N), 3163, 3246, 3283, 3337 (N—H). ^{1}H NMR (400.13 MHz, DMSO-d_6): δ_H 3.71 (3H, s, OCH_3), 4.44 (1H, s, 4-H), 6.84 (2H, d, *J* 8.8 Hz, 3′-H and 5′-H), 7.12 (2H, d, *J* 8.8 Hz, 2′-H and 6′-H), 7.23 (2H, s, NH_2), 7.29 (1H, dt, *J* 7.6 and 1.2 Hz, 9-H), 7.33 (1H, d, *J* 8.0 Hz, 7-H), 7.57 (1H, dt, *J* 7.8 and 1.6 Hz, 8-H), 7.90 (1H, dd, *J* 8.0 and 0.8 Hz, 10-H), 11.75 (1H, s, N—H).

3. Results and discussion

Although room-temperature ILs are ideal for most applications, handling and storage of these compounds, particularly their acidic variants, are tedious. Thus, developing solid salts with amphipathic character should be emphasized. These salts, despite their solid state above 100 °C, melt easily at lower temperatures when are used in organic reactions, since a considerable measure of their fusion enthalpy is provided by solvating the organic substrates of reaction mixtures. Our approach to prepare a new amphipathic complex salt (CS) is outlined in Scheme 1. The acid-base reaction between triethylamine and two equivalents of chlorosulfonic acid gave the IL triethylammonium chlorosulfonate **1**. Addition of this water-sensitive IL to an equimolar amount of 1,1,3,3-tetramethylguanidine in CH_2Cl_2 under moist air led to the formation of the complex salt [TMG-H][Et_3N-H][(HCl)(HSO_4)$_2$], which melts at 118 °C. The stoichiometric contents of one chloride ion and two bisulfate ions in the empirical formula of this salt were confirmed through separate titration measurements of the ions with Ag^+ and Ba^{2+} [35]. Dissolving a certain amount of the salt into aqueous $BaCl_2$ solution results in precipitating two equivalents of $BaSO_4$, implying that TMG has not been sulfonated by **1** and the sulfur content of the salt exists as bisulfate anion. Interestingly, the CS contains the ions of TMG·HCl and Et_3N·HCl, i.e. the salts with the moderate melting point temperatures of 210 °C and 255 °C, respectively. Certainly, the melting point depression of these simple salts is related to the stabilization of Cl^- by extensive H-bonding with bisulfate ions.

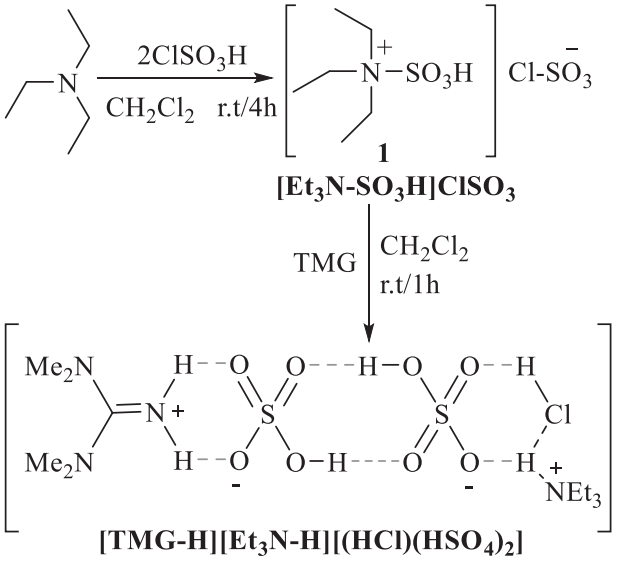

Scheme 1. The reaction steps for synthesis of the CS, [TMG-H][TEA-H][(HCl)(HSO_4)$_2$]

The FT-IR spectrum of the pure CS indicates a strong broad band peaking at 3377 cm^{-1} and a subsidiary broad shoulder at around 3190 cm^{-1} corresponding to O—H and N—H stretching vibrations. The split of these vibrations into two distinguishable bands suggests that certain, but different, H-bonds are involved in defining the structure of the CS. Interesting to notice are the bands (1191, 1058, and 879 cm^{-1}) appeared in the S═O stretching vibrations region [36]. The presence of these three bands indicates that the sulfate ions in the CS are no longer isolated ions but exist with less symmetry due to strong H-bonding with other species in the salt. In addition, the isolated SO_4^{2-} belongs to the higher symmetry point group (T_d), and only one vibrational band is expected for this symmetric ion in the S═O stretching region [37,38]. The deformation vibrations of SO_4^{2-} ions resulted in a moderate band at 595 cm^{-1} flanked by a small shoulder at 612 cm^{-1}. Other characteristic bands in the spectrum can be attributed to the C—N stretching (1120 cm^{-1}), CH_3 deformation (1470 cm^{-1}), N—H bending (1613 cm^{-1}), C═N stretching (1648 cm^{-1}), and the aliphatic C—H stretching (2940 and 2973 cm^{-1}) vibrations. The ^{1}H NMR spectrum of the CS in DMSO-d_6 exhibited a broad singlet peak in the downfield end at δ 9.82 due to the proton attached to triethylamine along with a singlet peak at δ 7.88, which is readily conceived as arising from the two equivalent protons of C═NH_2 group in the protonated TMG. Due to similar couplings with the adjacent N—H and CH_3 protons (*J* 6.8 Hz), the enantiotopic CH_2 protons in Et_3N-H appeared as a pentet peak at δ 3.08. It is worth noting that the four methyl groups of the TMG-H cation in the CS resonated as a singlet peak with the chemical shift (δ_H 2.91) close to that of pristine TMG (δ_H 2.73), indicating that neither of the two methylated nitrogen atoms are protonated. The preferred protonation of TMG at its sp^2-hybridized nitrogen atom allows the π-electrons and consequently the generated positive charge to be delocalized over the entire molecule. On the other hand, the protonation of TMG at either of the methylated nitrogen atoms would interrupt the resonance of its π-system. Therefore, TMG-H is too weak to neutralize the remaining acidic species of the CS. In other words, the HSO_4^- ions, instead of participating in the neutralization reactions, take part as structural units in a network of H-bonds by trapping the HCl molecule of the CS within their acidic H-bonds. These acids resulted in a broad peak with the integral of 3H at δ_H 5.94 ppm, which is a convincing evidence to confirm the structure of the CS. Because of its structural features, the CS is a solid acid as its 0.01 M solution in water has the pH = 2.

The thermal behavior of the CS was studied by thermogravimetric analysis (TGA) and differential scanning calorimetry (DSC) in the temperatures between 25 and 600 °C (Fig. 2). The TG curve of the CS exhibited an initial slight mass loss of ~ 6% up to 78 °C due to the evaporation of the moisture adsorbed by the salt. After this preliminary stage, the curve becomes almost a plateau up to 187 °C and then smoothly

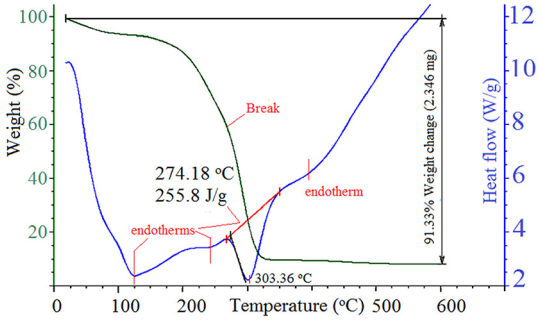

Fig. 2. The TGA and the DSC thermograms of the CS.

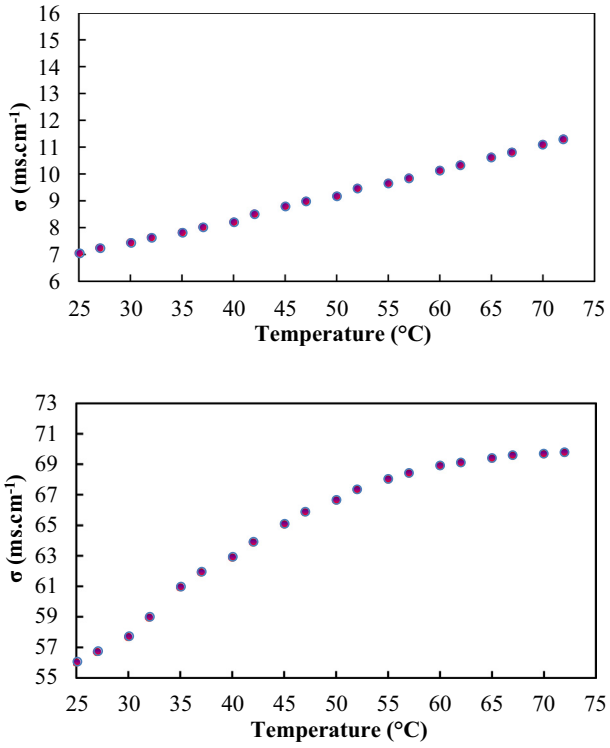

Fig. 3. Plots of conductivity against temperature (°C) for the CS in DMF (up) and in H_2O (down).

bends down until reaching the first degradation step. Evidently, none of the fragments has been vaporized within the early flattened domain of the TG curve, as the CS displayed the same FT-IR spectrum even after three successive cycles of melting and recrystallization. The early flat region in the TG curve corresponds to an endotherm in the DSC thermograph, peaking at 118 °C and coinciding with the melting point of the CS. Two consecutive degradation steps are observed in the TG curve, each corresponding to an endotherm in the DSC thermograph. The first degradation trace slides down with a steep slope from the onset point of 207 °C to reach a break at 274 °C from which the degradation of the CS continues (the second step) with even a steeper slope than the first step and ends at 320 °C. By the end of these steps, about 91% of the mass is lost and then the chars remaining from the CS are degraded smoothly associated with an endotherm in the DSC curve.

The CS exhibited a significant electric conductivity (EC) in water and DMF, reflecting its ionic characteristic. Fig. 3 demonstrates the plot of EC versus temperature for [TMG-H][TEA-H][(HCl)$(HSO_4)_2$] solutions in DMF and water, respectively. The following calculation was used to specify the conductivity of the CS in each of the solutions, where $\sigma'_{(t, CS)}$ denotes the EC contributed by the CS to its solution at a given temperature and the symbols $\sigma'_{(t, solu.)}$ and $\sigma'_{(t, solv.)}$ represent the ECs of the solution and the pure solvent at the same temperature, respectively.

$$\sigma'_{(t,CS)} = \sigma'_{(t,solu.)} - \sigma'_{(t,solv.)}$$

Obviously, the EC for the CS in water is an order of magnitude greater than in DMF. In other words, the CS ionizes much more in water than in DMF, giving a more concentrated solution of the charge carriers in water. Apparently, the complex macromolecular structure of the CS is somewhat preserved in DMF where it, because of possessing a great Stocks radii, has low mobility to take part efficiently in the EC. This could be justified by considering the fact that the EC of the CS in water increases with a steeper slope than in DMF while increasing the temperature. This observation can be rationalized in terms of the CS complete ionization in water, producing ions with smaller Stocks radii and faster mobility than the complex ions in DMF.

Based on the structural features of the CS, it was expected to have a remarkable catalytic activity in the acid demanding reactions. In this view, we decided to examine the CS as the catalyst in the synthesis of benzo[*b*]pyrans, pyrano[4,3-*b*]pyrans, pyrano[3,2-*c*]quinolones, and pyrido[2,3-*d*]pyrimidines via the three-component reactions of 4-hydroxycoumarin/ dimedone/ 4-hydroxy-6-methyl-2-pyrone/ 4-hydroxyquinolin-2-one/ or 6-aminouracil with malononitrile and arylaldehydes. To find the optimal conditions, the reaction between 4-chlorobenzaldehyde **2**, malononitrile **3**, and 4-hydroxycoumarin **4** was selected as the model to be tested in different solvents and different temperatures (Scheme 2). As shown in Table 2, the best result was obtained by running the model reaction at 70 °C using 10 mol% of [TMG-H][TEA-H][(HCl)$(HSO_4)_2$] as catalyst under solvent-free condition (entry 8). A striking observation in these experiments was the easy fusion and homogenization of the CS with the substrates near 50 °C. This easy fusion arises from the amphipatic character of the CS and causes the trial synthesis to be accomplished in fairly high yields within short reaction times under the solvent-free condition (entry 7). On the other hand, only a negligible yield of the model product was obtained by performing the reaction in the absence of any catalyst even within a prolonged time (up to 120 min) of heating in a polar solvent (entry 1). None of the basic components of the CS can be considered as active catalysts since the yields are negligible under homogeneous catalysis of Et_3N or TMG within comparable times at 70 °C (entries 2, 3). In contrast, the acidic constituents of the CS exhibited significant catalytic activities (entries 4, 5), however with less efficiencies than the CS itself, implying that the CS acts almost as an acid catalyst. It is worth noting that the catalytic activity of the CS is retained in polar hydroxyl solvents (entries 11,12) but diminishes by performing the trial reaction in some ordinary solvents (entries 13–15). One of the most advantages of [TMG-

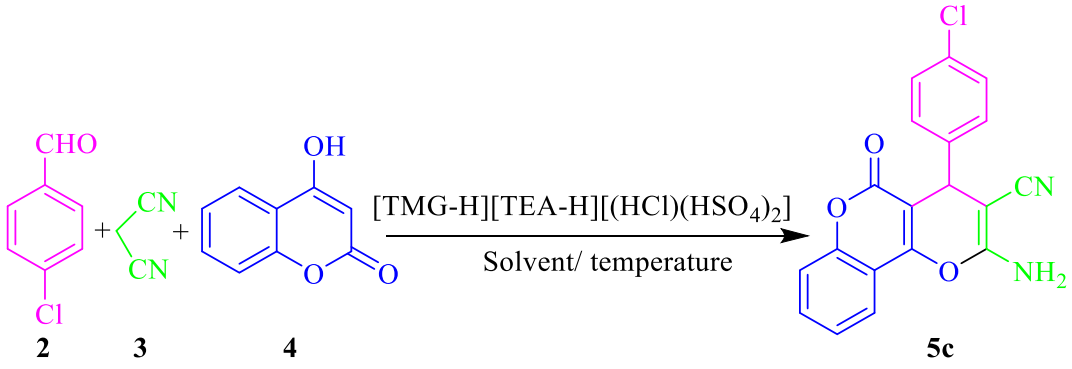

Scheme 2. Synthesis of 2-amino-4-(4-chlorophenyl)-3-cyano-4*H*,5*H*-pyrano[3,2-*c*][1]benzopyran-5-one as the model product

Table 2
Optimization of the conditions for the reaction of 4-hydroxycoumarin with malononitrile and 4-chlorobenzaldehyde in the presence of [TMG-H][TEA-H][(HCl)$(HSO_4)_2$].

Entry	Catalyst	Solvent	Temp (°C)	Time (min)	Yield (%)[a]
1	None	H_2O:CH_3OH	70	40	12
2	Et_3N	H_2O:CH_3OH	70	40	16
3	TMG	None	70	40	–
4	[Et_3N-H][HSO_4] (20 mol%)	None	70	40	77
5	[TMG-H][HSO_4] (20 mol%)	None	70	40	86
6	[TMG-H][TEA-H][(HCl)$(HSO_4)_2$](10 mol%)	None	r.t.	40	Trace
7	[TMG-H][TEA-H][(HCl)$(HSO_4)_2$](10 mol%)	None	50	40	88
8	**[TMG-H][TEA-H][(HCl)$(HSO_4)_2$](10 mol%)**	**None**	**70**	**12**	**92**
9	[TMG-H][TEA-H][(HCl)$(HSO_4)_2$](10 mol%)	None	100	12	92
10	[TMG-H][TEA-H][(HCl)$(HSO_4)_2$](25 mol%)	None	70	12	93
11	[TMG-H][TEA-H][(HCl)$(HSO_4)_2$](10 mol%)	H_2O	70	40	86
12	[TMG-H][TEA-H][(HCl)$(HSO_4)_2$](10 mol%)	CH_3OH	70	40	87
13	[TMG-H][TEA-H][(HCl)$(HSO_4)_2$](10 mol%)	CH_3CN	70	40	27
14	[TMG-H][TEA-H][(HCl)$(HSO_4)_2$](10 mol%)	CH_2Cl_2	70	40	Trace
15	[TMG-H][TEA-H][(HCl)$(HSO_4)_2$](10 mol%)	DMF	70	40	58

[a] Isolated yields. The parameters of the bold entry (8) were identified optimal.

H][TEA-H][(HCl)$(HSO_4)_2$] is that it can be separated from the reaction mixtures by aqueous extraction and evaporation of the solvent.

To explore the substrate scope of this method, a variety of substrates were employed in the reaction with malononitrile to yield the corresponding products (Scheme 3).

In all the syntheses, the desired products were obtained in fairly high yields within relatively short reaction times (Table 3). It was observed that the three-component reactions can be conducted efficiently by using various aromatic aldehydes containing either electron-withdrawing or electron-donating substituents.

A plausible mechanism for the catalysis action of [TMG-H][TEA-H][(HCl)$(HSO_4)_2$] in the above syntheses was outlined in Scheme 4. Certainly, the syntheses initiate by Knoevenagel condensation of the aldehyde with malononitrile, and the role of the CS in this nucleophilic reaction is to activate the aldehyde by protonation. The similar activation of the aldehyde-malononitrile condensate **10** by protonation with the CS facilitates its nucleophilic addition onto the third substrate to deliver the adduct **11**. This intermediate undergoes a Thorpe-Ziegler type cyclization through an intramolecular nucleophilic addition reaction, which is similarly catalyzed by protonation of the nitrile group. The last reaction is followed by a tautomerization to yield the final product.

To verify the efficiency of the present method, it was compared with some previously reported catalytic methods for the representative synthesis of **5c** (Table 4). As shown, [TMG-H][TEA-H][(HCl)$(HSO_4)_2$] proves itself as an alternative to the efficient catalysts reported for the model synthesis. Some of the previously reported catalysts are not as efficient as the CS (entries 1–4) and others are liquid, so cannot be handled easily (entry 6), or that operate at higher temperatures. In comparison with

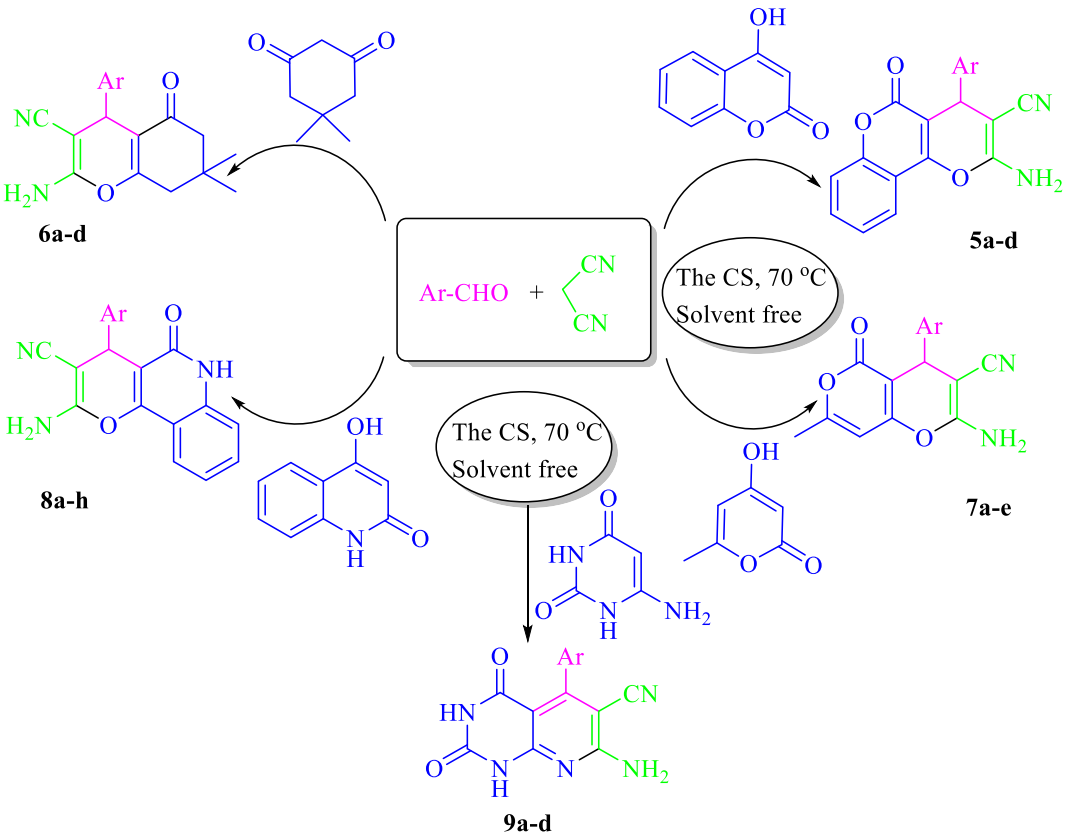

Scheme 3. Synthesis of benzo[*b*]pyran, pyrano[4,3-*b*]pyran, pyrano[3,2-*c*]quinolines and pyrido[2,3-*d*]pyrimidine derivatives catalyzed by [TMG-H][TEA-H][(HCl)$(HSO_4)_2$]

Table 3
Synthesis of benzo[*b*]pyrans (**5a-d, 6a-d**), pyrano[4,3-*b*]pyrans (**7a-e**), pyrano[3,2-*c*]quinolones (**8a-h**), and pyrido[2,3-*d*]pyrimidines (**9a-d**) under the optimized conditions.

Entry	Aldehyde	Product	Time (min)	Yield (%)[a]	Mp (°C)	
					Found	reported (ref.)
1	3-NO_2-C_6H_4	**5a**	10	89	259–261	263–265 [39]
2	4-NO_2-C_6H_4	**5b**	10	92	258–260	260–262 [39]
3	4-Cl-C_6H_4	**5c**	12	92	259–262	262–264 [39]
4	4-MeO-C_6H_4	**5d**	12	86	250–253	246–248 [39]
5	3-NO_2-C_6H_4	**6a**	10	92	210–212	213–214 [40]
6	4-NO_2-C_6H_4	**6b**	10	94	179–180	176–178 [40]
7	4-Cl-C_6H_4	**6c**	12	91	209–211	212–214 [40]
8	4-MeO-C_6H_4	**6d**	12	87	194–196	195–196 [41]
9	3-NO_2-C_6H_4	**7a**	10	91	232–234	234–236 [42]
10	4-NO_2-C_6H_4	**7b**	10	93	206–207	211–213 [43]
11	4-Cl-C_6H_4	**7c**	12	93	222–225	228–230 [44]
12	4-MeO-C_6H_4	**7d**	12	85	201–204	200–202 [43]
13	4-CHO-C_6H_4	**7e**	10	89	258–260	256–258 [44]
14	C_6H_5	**8a**	12	88	>300	297–299 [45]
15	2-Cl-C_6H_4	**8b**	14	84	297–298	294–296 [45]
16	4-Cl-C_6H_4	**8c**	14	92	>300	297–299 [45]
17	3-Br-C_6H_4	**8d**	14	79	>300	>300 [45]
18	4-NO_2-C_6H_4	**8e**	10	93	>300	>300 [45]
19	4-MeO-C_6H_4	**8f**	14	85	296–300	297–300 [44]
20	4-Me-C_6H_4	**8g**	14	90	>300	>300 [44]
21	2-thiophenaldehyde	**8h**	14	85	>300	>300 [44]
22	3-NO_2-C_6H_4	**9a**	10	93	>300	>300 [46]
23	4-NO_2-C_6H_4	**9b**	10	94	>300	>300 [46]
24	4-Cl-C_6H_4	**9c**	12	91	>300	>300 [26]
25	4-MeO-C_6H_4	**9d**	12	82	>300	>300 [46]

[a] Isolated yields.

similar recent methods, a slight quantity of the CS gives a comparable yield of the product **5c** within a short reaction time.

Different solubility of the CS and products in limited solvents facilitates their separation from each other and from the reaction mixtures by extraction, which provides promoting the synthetic protocol as a sustainable catalytic method. In this regard, the recyclability of the CS in the synthesis of **5c** under the optimized reaction conditions was studied. At the end of the synthesis, the CS was separated from the reaction mixture by adding water, decanting the supernatant aqueous extract from the crude solid product, and evaporating the aqueous extract. The purification of the CS can be monitored and facilitated by its solidification in the evaporation vessel. As displayed in Fig. 4, the CS can be recycled several times in the model reaction without any considerable decrease in its catalytic activity. The FT-IR spectrum of the freshly prepared CS and that collected after the third recycling are essentially identical.

4. Conclusion

The reaction of triethyl(sulfonyl)ammonium chlorosulfonate with an equimolar amount of 1,1,3,3-tetramethylguanidine in moist air gave a complex salt melting at 118 °C. Spectroscopic and chemical analysis of this salt is consistent with the structure composed of an HCl molecule trapped within a network of H-bonded HSO_4^- and the ammonium ions. ^{1}H NMR spectrum of this salt displayed that its tetramethylguanidine component was monocationic and was protonated only at 3-position. In fact, the salt is more acidic as its 0.01 M

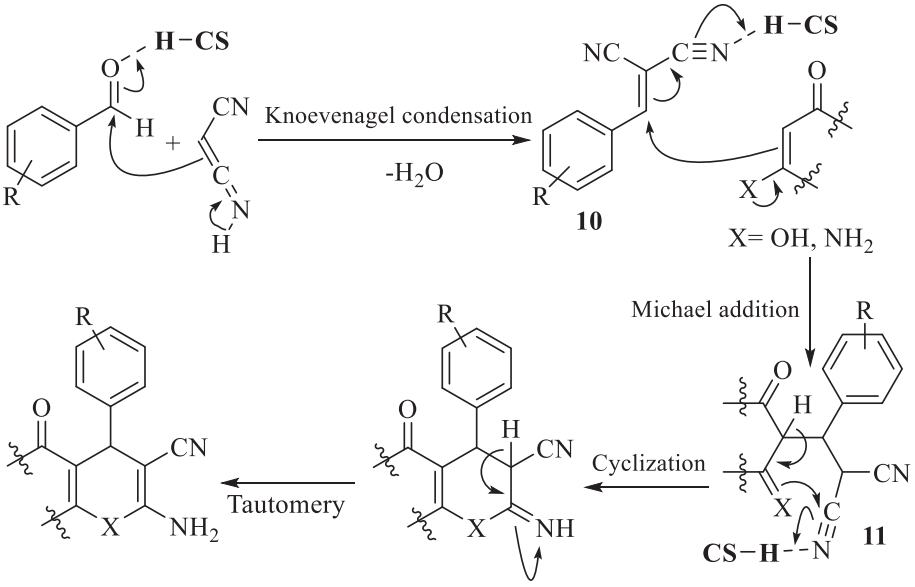

Scheme 4. A proposed mechanism for the catalysis action of [TMG-H][TEA-H][(HCl)$(HSO_4)_2$] in the syntheses

Table 4
A comparative catalytic efficiency of [TMG-H][TEA-H][$(HCl)(HSO_4)_2$] in the synthesis of **5c**.

Entry	Catalyst	Conditions	Time (min)	Yield (%)	Ref.
1	Diammonium hydrogen phosphate	H_2O:EtOH/r.t	120	85	[47]
2	(*S*)-Proline	H_2O:EtOH/reflux	120	78	[47]
3	Fe_3O_4@SiO_2/DABCO	H_2O/80 °C	35	87	[25]
4	MgO nano powder	H_2O/100 °C	120	86	[48]
5	[Sipim]HSO_4	Solvent-free/100 °C	30	95	[49]
6	$[H_3N^+–CH_2–CH_2–OH][CH_3COO^-]$	Solvent-free/r.t.	10	93	[50]
7	[TMG-H][TEA-H][$(HCl)(H_2SO_4)_2$]	Solvent-free/70 °C	12	92	This study

[Sipim] = silica-grafted *N*-propylimidazolium.

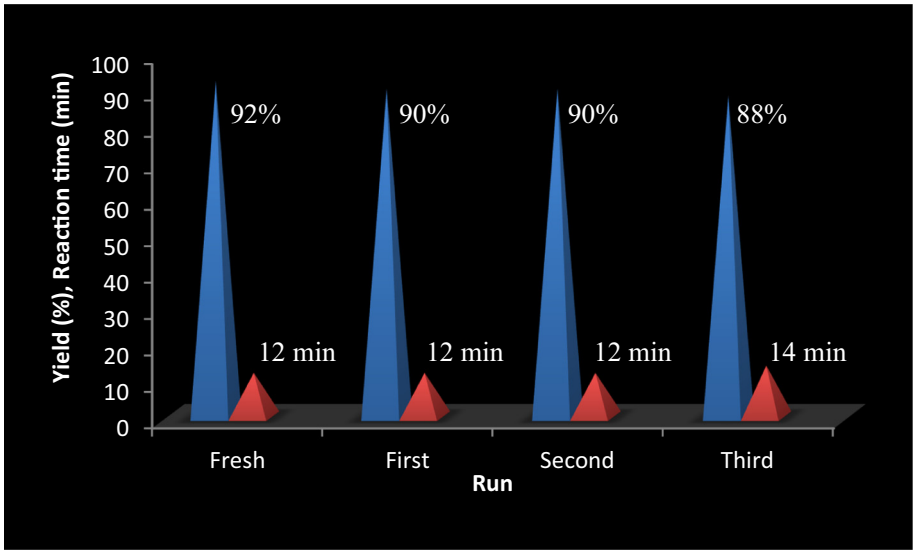

Fig. 4. Recyclability tests of [TMG-H][TEA-H][$(HCl)(HSO_4)_2$] in the synthesis of **5c**.

solution in water has the pH = 2. Accordingly, it was successfully examined as a homogeneous catalyst in the acid-demanding three-component synthesis of benzo[*b*]pyrans, pyrano[4,3-*b*]pyrans, pyrano[3,2-*c*]quinolones, and pyrido[2,3-*d*]pyrimidines. It is noteworthy that the salt is amphipatic, hence can be fused with the substrates on slight heating their mixture. As a result, all the syntheses were accomplished in a homogeneous phase at 70 °C to produce fairly high yields of the desired products. In addition, the acidic salt is reasonably stable in moist air for long times and can be stored and handled safely.

CRediT authorship contribution statement

Maedeh Saeedi Mirak-Mahaleh: Investigation, Writing - original draft. **Kurosh Rad-Moghadam:** Supervision, Conceptualization, Methodology, Writing - review & editing, Data curation.

Declaration of competing interest

The authors declare that have no conflict of interest with other people or organizations in relation to publication of this work.

Acknowledgements

The authors are grateful to the research council of University of Guilan for the supports of this work.

Appendix A. Supplementary data

Supplementary data to this article can be found online at https://doi.org/10.1016/j.molliq.2020.112989.

References

[1] M. Honarmand, A. Tzani, A. Detsi, Synthesis of novel multi-OH functionalized ionic liquid and its application as dual catalyst-solvent for the one-pot synthesis 4H-pyrans, J. Mol. Liq. 290 (2019) 111358, press https://doi.org/10.1016/j.molliq.2019.111358.
[2] B. Pegot, G. Vo-Thanh, D. Gori, A. Loupy, First application of chiral ionic liquids in asymmetric Baylis–Hillman reaction, Tetrahedron Lett. 45 (2004) 6425–6428, https://doi.org/10.1016/j.tetlet.2004.06.134.
[3] M.J. Earle, S.P. Katdare, K.R. Seddon, Paradigm Confirmed: the first use of ionic liquids to dramatically influence the outcome of chemical reactions, Org. Lett. 6 (2004) 707–710, https://doi.org/10.1021/ol036310e.
[4] A.N. Masri, M.I. Abdul Mutalib, W.Z.N. Yahya, N.F. Aminuddin, J.M. Leveque, Rapid esterification of fatty acid using dicationic acidic ionic liquid catalyst via ultrasonic-assisted method, Ultrason. Sonochem. 60 (2020) 104732, press https://doi.org/10.1016/j.ultsonch.2019.104732.
[5] K.N. Tiwari, S.R. Thakar, V. Kumar, S.M. Prabhakaran, Catalyst-free synthesis of 3-substituted-3-hydroxy-2-oxindoles by reaction of isatin and cyclic enaminone in water, Synth. Commun. 48 (2018) 2965–2972, https://doi.org/10.1080/00397911.2018.1525740.
[6] R.L. Vekariya, A review of ionic liquids: applications towards catalytic organic transformations, J. Mol. Liq. 227 (2017) 44–60, https://doi.org/10.1016/j.molliq.2016.11.123.
[7] A. El-Harairy, B. Lai, L. Vaccaro, M. Li, Y. Gu, A sulfone-containing imidazolium-based Brønsted acid ionic liquid catalyst enables replacing dipolar aprotic solvents with butyl acetate, Adv. Synth. Catal. 361 (2019) 3342–3350.
[8] Y. Xiao, X. Huang, The physicochemical properties of a room-temperature liquidus binary ionic liquid mixture of [HNMP][CH_3SO_3]/[Bmim]Cl and its application for fructose conversion to 5-hydroxymethylfurfural, RSC Adv. 8 (2018) 18784–18791, https://doi.org/10.1039/C8RA03604G.
[9] S. Thawarkar, N.D. Khupse, D.R. Shinde, A. Kumar, Understanding the behavior of mixtures of protic-aprotic and protic-protic ionic liquids: conductivity, viscosity, diffusion coefficient and iconicity, J. Mol. Liq. 276 (2019) 986–994, https://doi.org/10.1016/j.molliq.2018.12.024.
[10] M. Antonietti, D. Kuang, B. Smarsly, Y. Zhou, Ionic liquids for the convenient synthesis of functional nanoparticles and other inorganic nanostructures, Angew. Chem. Int. Ed. 43 (2004) 4988–4992, https://doi.org/10.1002/anie.200460091.
[11] B. Wu, Y. Liu, Y. Zhang, H. Wang, Probing intermolecular interactions in ionic liquid–water mixtures by near-infrared spectroscopy, Chem. Eur. J. 15 (2009) 6889–6893, https://doi.org/10.1002/chem.200802742.

[12] S.Y. Kalurazi, K. Rad-Moghadam, Sh. Moradi, Efficient catalytic application of a binary ionic liquid mixture in the synthesis of novel spiro[4*H*-pyridine-oxindoles], New J. Chem. 41 (2017) 10291–10298, https://doi.org/10.1039/C7NJ01858D.
[13] L. Chen, S. Bao, L. Yang, X. Zhang, B. Li, Y. Li, Cheap thiamine hydrochloride as efficient catalyst for synthesis of 4*H*-benzo[*b*]pyrans in aqueous ethanol, Res. Chem. Intermed. 43 (2017) 3883–3891, https://doi.org/10.1007/s11164-016-2843-x.
[14] Á. Magyar, Z. Hell, One-pot, three-component, selective synthesis of the polyfunctionalized 4*H*-pyran and 4*H*-benzo[*b*]pyran derivatives in the presence of a highly efficient molecular sieve-supported zinc catalyst, Green Process. Synth. 7 (2017) 316–322, https://doi.org/10.1515/gps-2017-0083.
[15] K.D. Upadhyay, N.M. Dodia, R.C. Khunt, R.S. Chaniara, A.K. Shah, Synthesis and biological screening of pyrano[3,2-*c*]quinoline analogues as anti-inflammatory and anticancer agents, ACS Med. Chem. Lett. 9 (2018) 283–288, https://doi.org/10.1021/acsmedchemlett.7b00545.
[16] P. Kumari, Ch. Narayana, Sh. Dubey, A. Gupta, R. Sagar, Stereoselective synthesis of natural product inspired carbohydrate fused pyrano[3,2-*c*]quinolones as antiproliferative agents, Org. Biomol. Chem. 16 (2018) 2049–2059, https://doi.org/10.1039/C7OB03186F.
[17] S. Moradi, M.A. Zolfigol, M. Zarei, D.A. Alonso, A. Khoshnood, A. Tajally, An efficient catalytic method for the synthesis of pyrido[2,3-*d*]pyrimidines as biologically drug candidates by using novel magnetic nanoparticles as a reusable catalyst, Appl. Organomet. Chem. 32 (2018), e4043. https://doi.org/10.1002/aoc.4043.
[18] H. Cairns, D. Cox, K. Gould, A. Ingall, J. Suschitzky, New antiallergic pyrano[3,2-*g*]quinoline-2,8-dicarboxylic acids with potential for the topical treatment of asthma, J. Med. Chem. 28 (1985) 1832–1842, https://doi.org/10.1021/jm00150a014.
[19] M.S. Mohamed, S.M. Awad, A.I. Sayed, Synthesis of certain pyrimidine derivatives as antimicrobial agents and anti-inflammatory agents, Molecles 15 (2010) 1882–1890, https://doi.org/10.3390/molecules15031882.
[20] M.M. Gineinah, M.N.A. Nasr, S.M.I. Badr, W.M. El-Husseiny, Synthesis and antitumor activity of new pyrido[2,3-*d*]pyrimidine derivatives, Med. Chem. Res. 22 (2013) 3943–3952, https://doi.org/10.1007/s00044-012-0396-0.
[21] H.J. Zhang, S.B. Wang, X. Wen, J.Z. Li, Z.S. Quan, Design, synthesis, and evaluation of the anticonvulsant and antidepressant activities of pyrido[2,3-*d*]pyrimidine derivatives, Med. Chem. Res. 25 (2016) 1287–1298, https://doi.org/10.1007/s00044-016-1559-1.
[22] Z.-Q. Xu, K. Pupek, W.J. Suling, L. Erache, M.T. Flavin, Pyranocoumarin, a novel anti-TB pharmacophore: synthesis and biological evaluation against Mycobacterium tuberculosis, Bioorg. Med. Chem. 14 (2006) 4610–4626, https://doi.org/10.1016/j.bmc.2006.02.017.
[23] N.L. Colbry, E.F. Elslager, L.M. Werbel, Folate antagonists. Synthesis and antimalarial properties of 2,4-diamino-6-(benzylamino)pyrido[3,2-*d*]pyrimidines, J. Med. Chem. 28 (1985) 248–252, https://doi.org/10.1021/jm00380a018.
[24] A. Kumar, R.A. Maurya, S.A. Sharma, P. Ahmad, A.B. Singh, G. Bhatia, A.K. Srivastava, Pyranocoumarins: a new class of anti-hyperglycemic and anti-dyslipidemic agents, Bioorg. Med. Chem. Lett. 19 (2009) 6447–6451, https://doi.org/10.1016/j.bmcl.2009.09.031.
[25] J. Davarpanah, A.R. Kiasat, S. Noorizadeh, M. Ghahremani, Nano magnetic double-charged diazoniabicyclo[2.2.2]octane dichloride silica hybrid: synthesis, characterization, and application as an efficient and reusable organic–inorganic hybrid silica with ionic liquid framework for one-pot synthesis of pyran annulated heterocyclic compounds in water, J. Mol. Catal. A Chem. 376 (2013) 78–89, https://doi.org/10.1016/j.molcata.2013.04.020.
[26] P. Bhattacharyya, S. Paul, A.R. Das, Facile synthesis of pyridopyrimidine and coumarin fused pyridine libraries over a Lewis base-surfactant-combined catalyst TEOA in aqueous medium, RSC Adv. 3 (2013) 3203–3208, https://doi.org/10.1039/C3RA23254A.
[27] V.L. Rechac, F.G. Cirujano, A. Corma, F.X. Llabrés i Xamena, Diastereoselective synthesis of pyranoquinolines on zirconium-containing UiO-66 metal-organic frameworks, Eur. J. Inorg. Chem. 2016 (2016) 4512–4516, https://doi.org/10.1002/ejic.201600372.
[28] F. Asghari-Haji, K. Rad-Moghadam, N.O. Mahmoodi, T. Tonekaboni, N. Rahimi, Cobalt ferrite encapsulated in a zwitterionic chitosan derived shell: an efficient nanomagnetic catalyst for three-component syntheses of pyrano[3,2-*c*]quinolines and spiro-oxindoles, Appl. Organomet. Chem. 31 (2017) 3891–3902, https://doi.org/10.1002/aoc.3891.
[29] F. Jalili, M. Zarei, M.A. Zolfigol, S. Rostamnia, A.R. Moosavi-Zare, SBA-15/PrN$(CH_2PO_3H_2)_2$ as a novel and efficient mesoporous solid acid catalyst with phosphorous acid tags and its application on the synthesis of new pyrimido[4,5-b]quinolones and pyrido[2,3-d]pyrimidines via anomeric based oxidation, Microporous Mesoporous Mater. 294 (2020) 109865, in press https://doi.org/10.1016/j.micromeso.2019.109865.
[30] B. Mirhosseini-Eshkevari, M. Esnaashari, M.A. Ghasemzadeh, Novel Brönsted acidic ionic liquids confined in UiO-66 nanocages for the synthesis of dihydropyrido[2,3-d]pyrimidine derivatives under solvent-free conditions, ACS Omega 4 (2019) 10548–10557, https://doi.org/10.1021/acsomega.9b00178.
[31] T. Farahmand, S. Hashemian, A. Sheibani, Efficient one-pot synthesis of pyrano[2,3-*d*]pyrimidinone and pyrido[2,3-*d*]pyrimidine derivatives by using of Mn-ZIF-8@ZnTiO3 nanocatalyst, J. Mol. Struct. 1206 (2020) 127667, press https://doi.org/10.1016/j.molstruc.2019.127667.
[32] X.S. Wang, Z.S. Zeng, D.Q. Shi, S.J. Tu, X.Y. Wei, Z.M. Zong, Three-component, one-pot synthesis of pyrido[2,3-*d*]pyrimidine derivatives catalyzed by KF-alumina, Synth. Commun. 35 (2005) 1921–1927, https://doi.org/10.1081/SCC-200064984.
[33] D.Q. Shi, Y. Zhou, H. Liua, An efficient synthesis of pyrido[2,3-*d*]pyrimidine derivatives in ionic liquid, J. Heterocycl. Chem. 47 (2010) 131–135, https://doi.org/10.1002/jhet.281.
[34] A. Zare, A.R. Moosavi-Zare, M. Merajoddin, M.A. Zolfigol, T. Hekmat-Zadeh, A. Hasaninejad, A. Khazaei, M. Mokhlesi, V. Khakyzadeh, F. Derakhshan-Panah, M.H. Beyzavi, E. Rostami, A. Arghoon, R. Roohandeh, Ionic liquid triethylamine-bonded sulfonic acid {[Et_3N–SO_3H]Cl} as a novel, highly efficient and homogeneous catalyst for the synthesis of *β*-acetamido ketones, 1,8-dioxo-octahydroxanthenes and 14-aryl-14H-dibenzo[*a,j*]xanthenes, J. Mol. Liq. 167 (2012) 69–77, https://doi.org/10.1016/j.molliq.2011.12.012.
[35] D.A. Skoog, D.M. West, F.J. Holler, Fundamentals of Analytical Chemistry, 7th ed. Thomson Learning, Inc., USA, 1996.
[36] C.J. Serna, J.L. White, S.L. Hem, Anion-aluminum hydroxide gel interactions, Soil Sci. Soc. Am. J. 42 (1977) 1009–1013, https://doi.org/10.2136/sssaj1977.03615995004100050041x.
[37] R.L. Parfitt, R.S.C. Smart, The mechanism of sulfate adsorption on iron oxides, Soil Sci. Soc. Am. J. 42 (1978) 48–50, https://doi.org/10.2136/sssaj1978.03615995004200010011x.
[38] P.K. Mandal, T.K. Mandal, Anion water in gypsum ($CaSO_4.2H_2O$) and hemihydrate ($CaSO_4.1/2H_2O$), Cem. Concr. Res. 32 (2002) 313–316, https://doi.org/10.1016/S0008-8846(01)00675-5.
[39] S. Khodabakhshi, B. Karami, Kh. Eskandari, S.J. Hoseini, Titanium dioxide nanowires as green and heterogeneous catalysts for the synthesis of novel pyranocoumarins, C. R. Chimie 17 (2014) 35–40, https://doi.org/10.1016/j.crci.2013.05.005.
[40] P. Sharma, M. Gupta, R. Kant, V.K. Gupta, One-pot synthesis of various 2-amino-4*H*-chromene derivatives using a highly active supported ionic liquid catalyst, RSC Adv. 6 (2016) 32052–32059, https://doi.org/10.1039/C6RA06523F.
[41] J. Yang, Sh. Liu, H. Hu, Sh. Ren, A. Ying, One-pot three-component synthesis of tetrahydrobenzo[*b*]pyrans catalyzed by cost-effective ionic liquid in aqueous medium, Chin. J. Chem. Eng. 23 (2015) 1416–1420, https://doi.org/10.1016/j.cjche.2015.04.020.
[42] E.V. Stoyanov, I.C. Ivanov, D. Heber, General method for the preparation of substituted 2-amino-4*H*,5*H*-pyrano[4,3-*b*]pyran-5-ones and 2-amino-4*H*-pyrano[3,2-*c*]pyridine-5-ones, Molecules 5 (2000) 19–32, https://doi.org/10.3390/50100019.
[43] A. Shaabani, S. Samadi, Z. Badri, A. Rahmati, Ionic liquid promoted efficient and rapid one-pot synthesis of pyran annulated heterocyclic systems, Catal. Lett. 104 (2005) 39–43, https://doi.org/10.1007/s10562-005-7433-2.
[44] N.G. Khaligh, 4-(Succinimido)-1-butane sulfonic acid as a Brönsted acid catalyst for synthesis of pyrano[4,3-*b*]pyran derivatives under solvent-free conditions, Chin. Chem. Lett. 26 (2015) 26–30, https://doi.org/10.1016/j.cclet.2014.10.009.
[45] Z. Tashrifi, K. Rad-Moghadam, M. Mehrdad, Catalytic performance of a new Brønsted acidic oligo(ionic liquid) in efficient synthesis of pyrano[3,2-*c*]quinolines and pyrano[2,3-d]pyrimidines, J. Mol. Liq. 248 (2017) 278–285, https://doi.org/10.1016/j.molliq.2017.10.065.
[46] Sh. Abdolmohammadi, S. Balalaie, An efficient synthesis of pyrido[2,3-*d*]pyrimidine derivatives via one-pot three-component reaction in aqueous media, Int. J. Org. Chem. 2 (2012) 7–14, https://doi.org/10.4236/ijoc.2012.21002.
[47] S. Abdolmohammadi, S. Balalaie, Novel and efficient catalysts for the one-pot synthesis of 3,4-dihydropyrano[c]chromene derivatives in aqueous media, Tetrahedron Lett. 48 (2007) 3299–3303, https://doi.org/10.1016/j.tetlet.2007.02.135.
[48] S.J. Roudbaraki, S. Sheik Mansoor, M. Ghashang, Aqueous media synthesis of pyrano[3,2-c]chromen derivatives using magnesium oxide nanoparticles as a recyclable catalyst, Polycycl. Aromat. Comp. (2019) https://doi.org/10.1080/10406638.2019.1576746in press.
[49] Kh. Niknam, A. Piran, Silica-grafted ionic liquids as recyclable catalysts for the synthesis of 3,4-dihydropyrano[*c*]chromenes and pyrano[2,3-*c*]pyrazoles, Green and Sustainable Chemistry 3 (2013) 1–8, https://doi.org/10.4236/gsc.2013.32A001.
[50] H.R. Shaterian, M. Honarmand, Task-specific ionic liquid as the recyclable catalyst for the rapid and green synthesis of dihydropyrano[3,2-*c*]chromene derivatives, Synth. Commun. 41 (2011) 3573–3581, https://doi.org/10.1080/00397911.2010.519594.